Supporting Information for

Facile Synthesis of Ag/Agcl Hybrid Nanostructures with Tunable Morphologies and Compositions as Advanced Visible Light Plasmonic Photocatalysts

Aasim Shahzad, Woo-Sik Kim* and Taekyung Yu*

Department of Chemical Engineering, College of Engineering, Kyung Hee University, Youngin, 446-701, Korea

E-mail: tkyu@khu.ac.kr (T. Yu) and wskim@khu.ac.kr (W.-S. Kim)

Table S1. Elemental composition of Ag and Cl in Ag/AgCl nanohybrids.

Nanoparticles	Atomic % of Ag	Atomic % of Cl	Atomic ratio, Ag:AgCl[a]	Reduction % of Ag[b]
AgCl	51.45	48.55	0.05	5.64
Ag/AgCl-0.1	66.58	33.42	0.99	49.80
Ag/AgCl-0.3	76.58	23.42	2.27	69.42
Ag/AgCl-0.5	80.44	19.56	3.112	75.68
Ag/AgCl-1.0	92.58	7.42	11.47	91.98
Ag/AgCl-1.5	96.37	3.63	25.54	96.23
Ag/AgCl-2.0	97.41	2.59	36.61	97.34

[a]Atomic ratio of Ag:AgCl = (A-B)/B
[b]Reduction % of Ag = (A-B)/A, (where A is the atomic % of Ag and B is the atomic %of Cl).

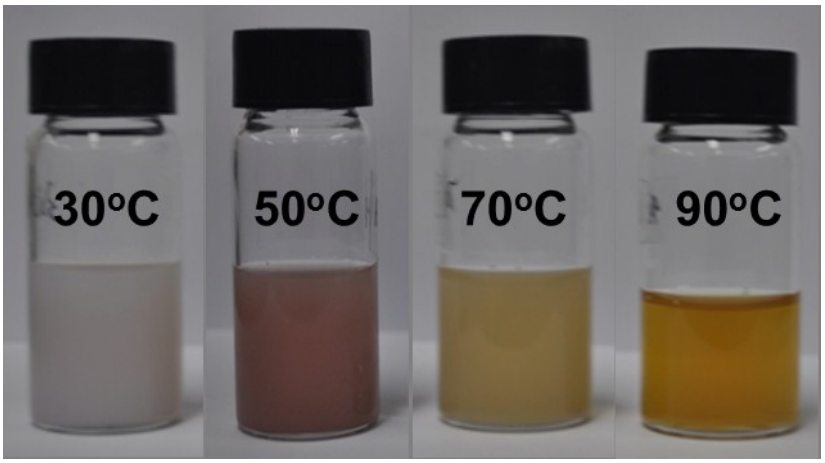

Figure S1. Optical photographs of the aqueous suspensions of the synthesized AgCl nanoparticles at different reaction temperatures, as shown in Figures 1a−d.

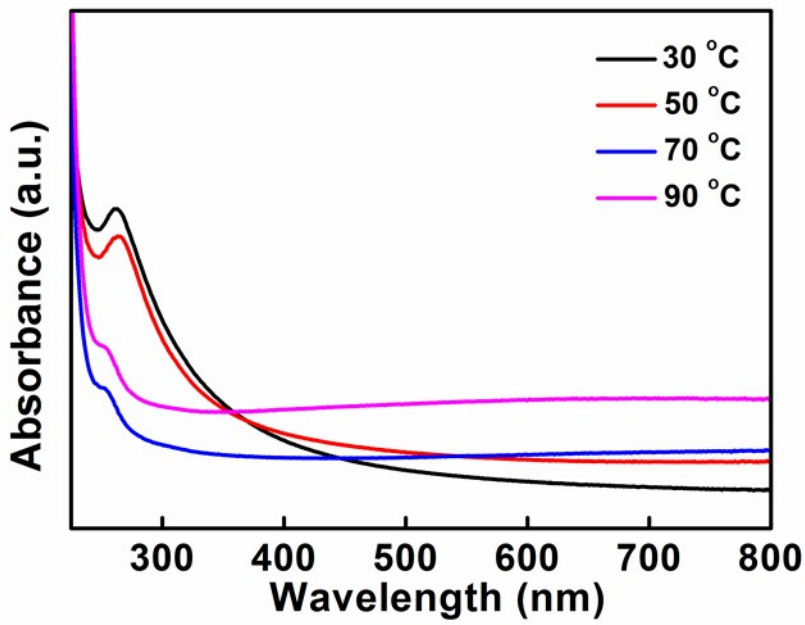

Figure S2. Absorption spectra of the AgCl nanoparticles, as shown in Figures 1a−d.

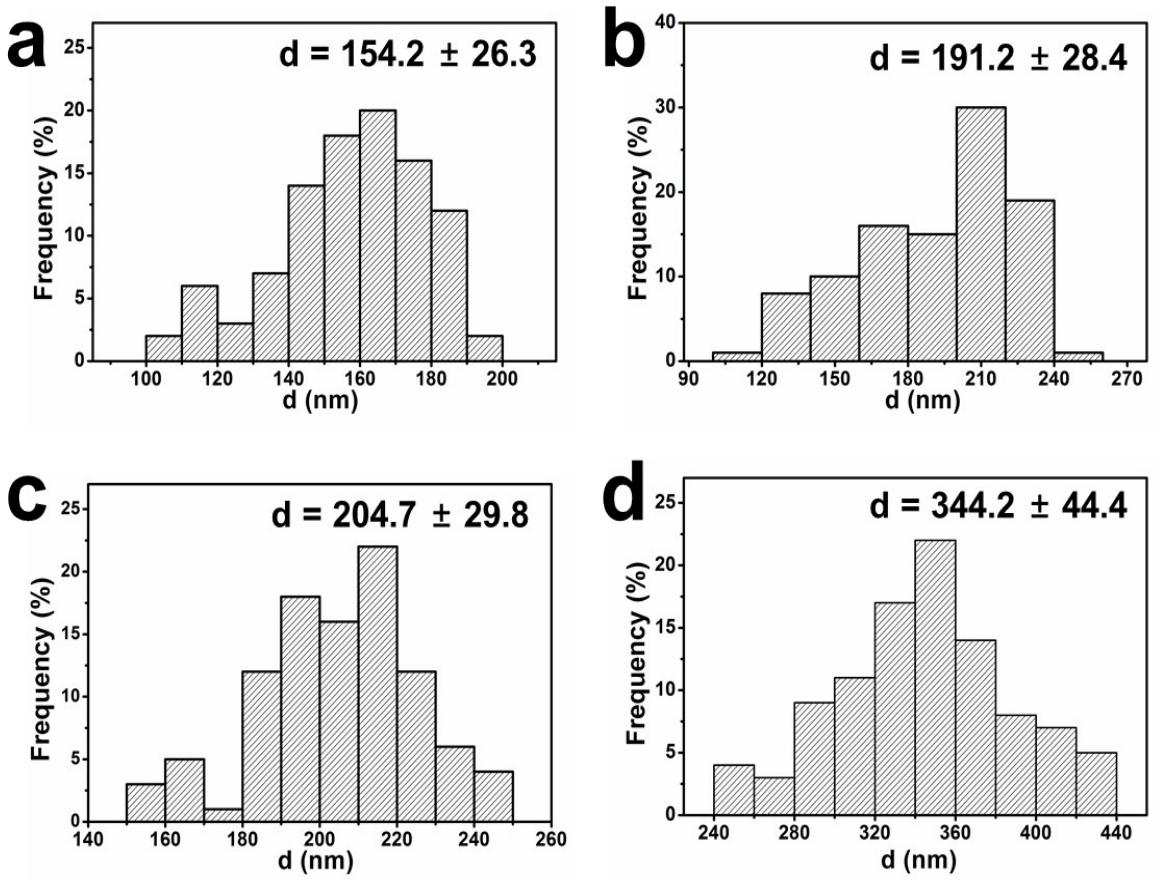

Figure S3. Particle size distributions of AgCl nanoparticles, as shown in Figures 1a−d; (a) 30 °C, (b) 50 °C , (c) 70 °C, and (d) 90 °C, respectively.

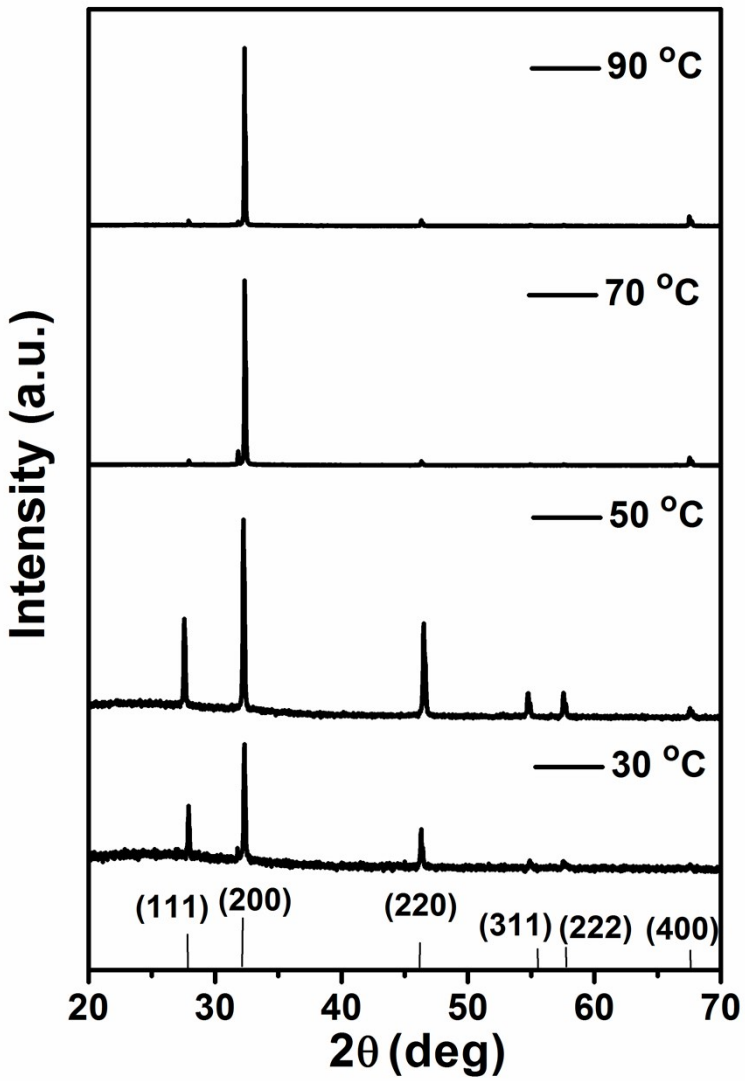

Figure S4. XRD pattern of AgCl nanoparticles, as shown in Figures 1a−d.

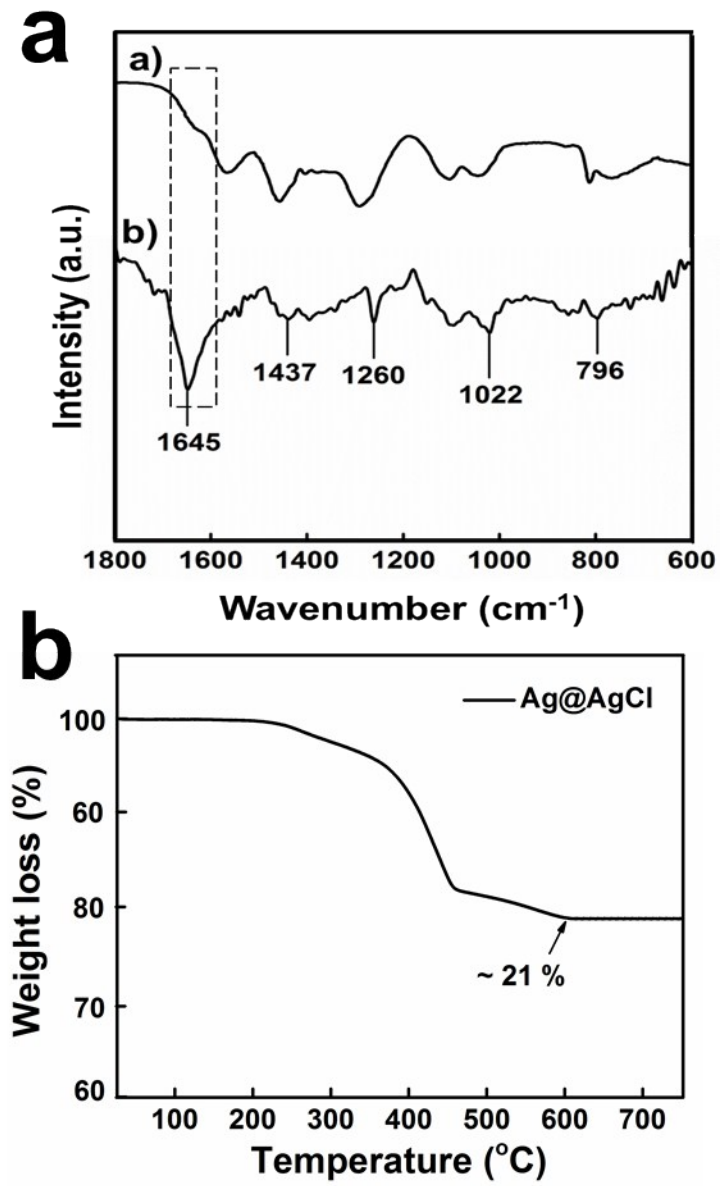

Figure S5. (a) FT-IR spectra; a) PEI, and b) PEI-stabilized AgCl nanoparticles. (b) TGA thermogram of AgCl nanoparticles, respectively,: samples prepared under same conditions as shown in Figure 1a.

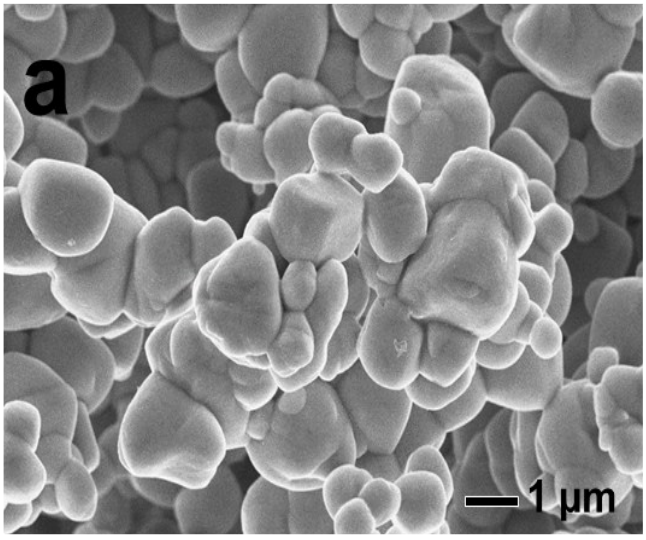

Figure S6. SEM image of AgCl nanoparticles prepared under the same conditions shown in Figure 1a, except that the reaction was conducted in the absence of PEI.

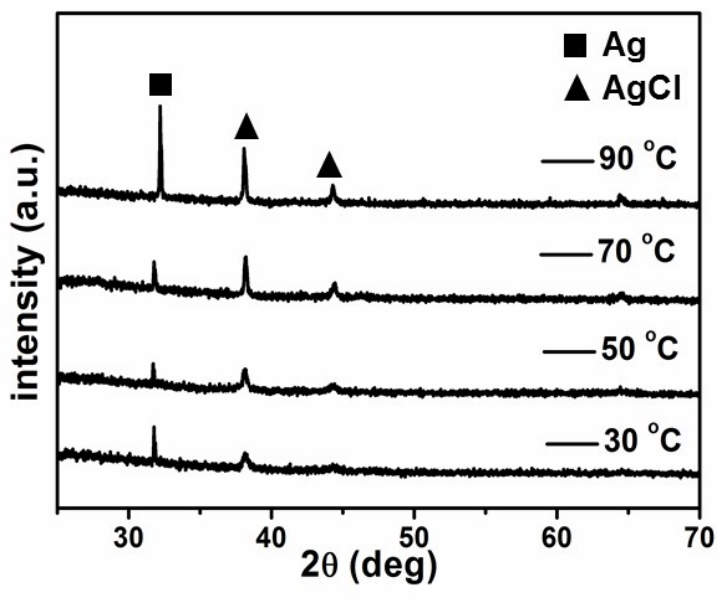

Figure S7. XRD patterns of the Ag/AgCl hybrid nanostructures synthesized by reacting the AgCl nanoparticles (Figures 1a−b, respectively) with 2.0 mL of $NaBH_4$ (10 mM).

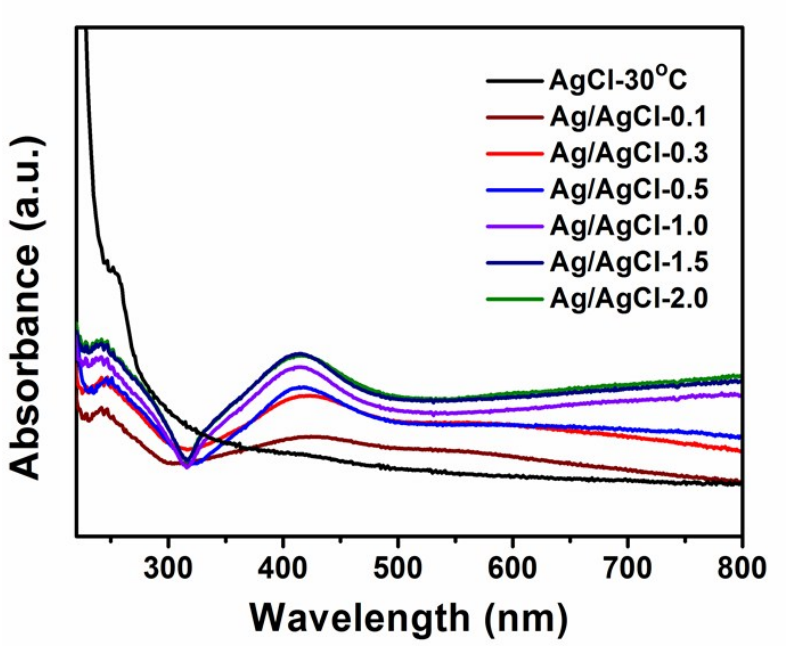

Figure S8. UV-vis absorption spectra of the AgCl semi-sphere and the Ag/AgCl hybrid nanostructures, as shown in Figures 3a−f.

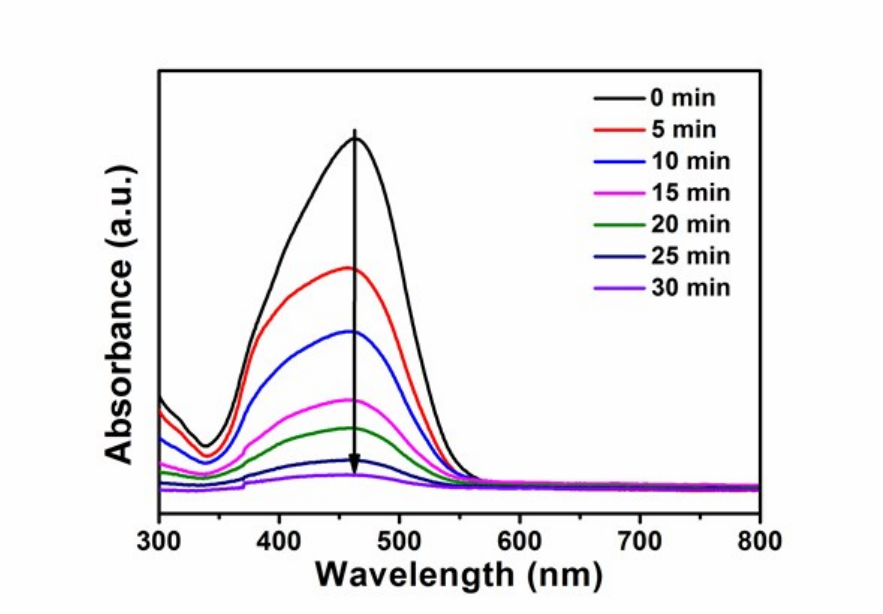

Figure S9. UV-vis absorption spectra for photocatalytic degradation of MO molecules using Ag/AgCl-0.5 under visible light irradiation.

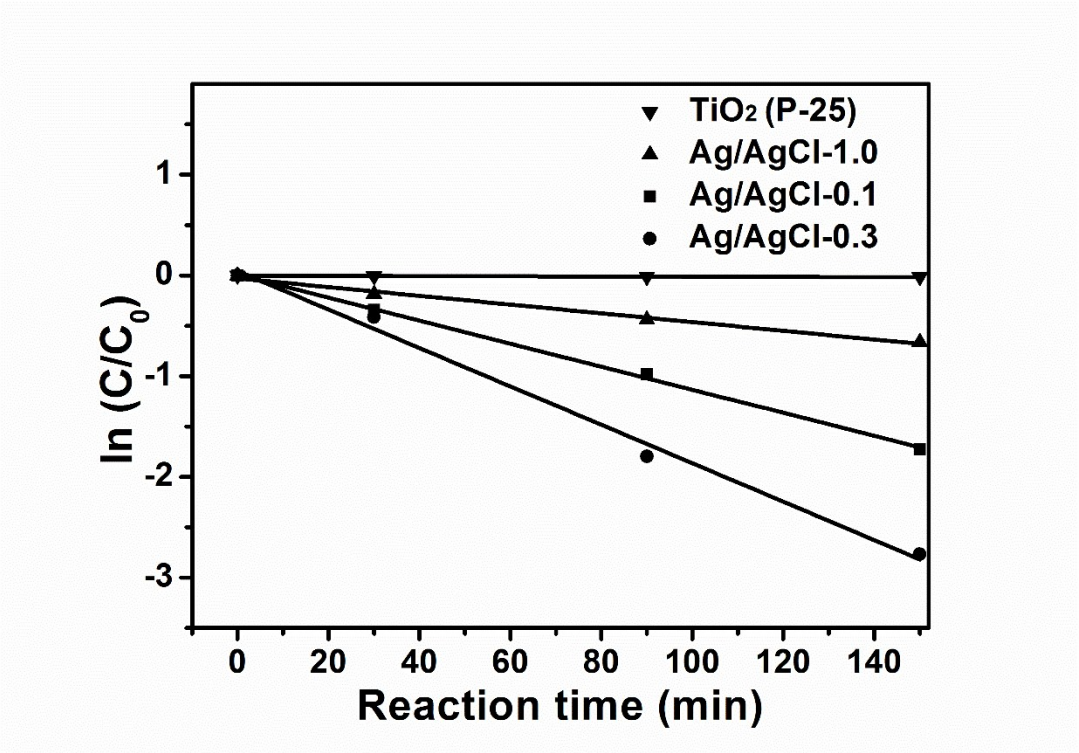

Figure S10. Kinetic plots of $\ln(C/C_0)$ against the reaction time for MO degradation using different photocatalysts.